Bioorganic & Medicinal Chemistry 19 (2011) 134–144

Contents lists available at ScienceDirect

Bioorganic & Medicinal Chemistry

journal homepage: www.elsevier.com/locate/bmc

Synthesis and evaluation of β-carboline derivatives as potential monoamine oxidase inhibitors

J. Reniers [a], S. Robert [b], R. Frederick [a], B. Masereel [b], S. Vincent [c], J. Wouters [a,*]

[a] Drug Design and Discovery Center, Laboratoire de Chimie Biologique Structurale, Facultés Universitaires Notre-Dame de la Paix, Namur, Belgium
[b] Drug Design and Discovery Center, Département de Pharmacie, Facultés Universitaires Notre-Dame de la Paix, Namur, Belgium
[c] Laboratoire de Chimie Bio-Organique, Facultés Universitaires Notre-Dame de la Paix, Namur, Belgium

ARTICLE INFO

Article history:
Received 5 August 2010
Revised 17 November 2010
Accepted 18 November 2010
Available online 25 November 2010

Keywords:
β-Carboline
MAO inhibition
Docking
X-ray

ABSTRACT

Previous studies have shown that harmine is a reversible inhibitor of human monoamine oxidase A (MAO-A). Moreover, the crystal structure of human MAO-A in complex with harmine has been recently solved. This crystal structure shows that close to the methoxy group of the harmine moiety, a lipophilic pocket is left vacant within the binding site of human MAO-A. Our objective was to optimize the β-carboline series against human MAO-A in order to explore this pocket. Therefore, a series of β-carboline derivatives has been synthesized. The compounds were evaluated for their human monoamine oxidase A and B inhibitory potency and their K_i values were estimated. The results show that O-alkylated compounds with lipophilic groups like cyclohexyl, phenyl and aliphatic chains increase the inhibition of MAO-A compared to harmine. Compound **3e**, with the trifluorobutyloxy group, was the most active of this series, with a K_i against MAO-A of 3.6 nM. Molecular docking studies show that the trifluorobutyloxy chain occupies the hydrophobic pocket vacant with harmine. The O-alkylated compounds are less active on MAO-B than on MAO-A. However, several compounds show a better inhibition on MAO-B compared to harmine. Compound **3f**, with the cyclohexylmethoxy chain, displayed the best inhibitory activity against MAO-B with a K_i value of 221.6 nM. This cyclohexyl bearing analogue is also a potent MAO-A inhibitor with a K_i value of 4.3 nM. Molecular docking studies show that the cyclohexyl chain also occupies a hydrophobic pocket but in different ways in MAO-A or MAO-B.

1. Introduction

Monoamine oxidase (MAO) is a flavoenzyme with the flavin adenine dinucleotide (FAD) covalently bound to a cysteine residue by an 8α-(*S*-cysteinyl)-riboflavin linkage. The enzyme is anchored to the mitochondrial outer membrane of neuronal, glial and several other cell types. It catalyzes the oxidative deamination of biogenic and xenobiotic amines to the corresponding aldehyde and ammonia in the periphery as well as in the central nervous system.[1] In mammals, MAO exists in two isoforms, MAO-A and MAO-B. They are dimeric in their membrane bound forms. MAO-B shares 70% of the amino acid sequence of MAO-A and, in particular, the active centers of both enzymes are very similar.[2] However, they differ with respect to distribution in body's tissues, and substrate/inhibitor specificity. MAO-A preferentially catalyzes the deamination of serotonin, adrenaline and noradrenaline and is selectively inhibited by clorgyline and moclobemide; MAO-B preferentially catalyzes the deamination of β-phenylethylamine and benzylamine and is irreversibly inhibited by selegiline.[3–5] In vitro, dopamine and tyramine are deaminated by both isoforms, but human dopamine is preferentially metabolized by MAO-B.

MAO-A and MAO-B are attractive targets for therapeutic intervention. MAO-A inhibitors are prescribed for the treatment of mental depression and anxiety.[6] MAO-B inhibitors are used with L-DOPA and/or dopamine agonists in the symptomatic treatment of Parkinson's disease.[7,8]

Most current monoamine oxidase inhibitors lead to side effects by a lack of affinity and selectivity towards one of the isoforms. So, it remains fundamental to design new more potent, reversible and selective inhibitors of MAO-A and MAO-B. With this aim in view, we started the design and the synthesis of β-carboline derivatives structurally related to harmine.

Harmine is a reversible MAO-A inhibitor.[9] Recently, the crystal structure of human MAO-A in complex with harmine has been solved.[10] The cocrystal structure (2Z5X.pdb) shows a lipophilic pocket formed by VAL93, LEU97, PHE108, ALA111, PHE208, CYS323 and ILE325 which is unoccupied with the methoxy group of harmine. So, we considered harmine as the starting point for the design of novel and more potent MAO-A inhibitors.

* Corresponding author. Tel.: +32 081 724550; fax: +32 081 725440.
E-mail address: johan.wouters@fundp.ac.be (J. Wouters).

0968-0896/$ - see front matter © 2010 Elsevier Ltd. All rights reserved.
doi:10.1016/j.bmc.2010.11.041

2. Results and discussion

2.1. Structure-based rational design

In the cocrystal structure (2Z5X.pdb), harmine is located in the active center cavity of the enzyme MAO-A. It interacts with TYR69, ASN181, PHE208, VAL210, GLN215, CYS323, ILE325, ILE335, LEU337, PHE352, TYR407, TYR444 and FAD[10] (Fig. 1a). Seven water molecules occupy the space between the inhibitor and these groups. Both nitrogen atoms of harmine establish also hydrogen bonds with two water molecules. Furthermore, pyridine function is stabilized with the aromatic cage (TYR407, TYR444 and FAD) by π–π interaction. The amide group of the GLN215 side chain interacts tightly with harmine by a π–π interaction. Moreover, nearby the methoxy group of the harmine, a lipophilic pocket formed by VAL93, LEU97, PHE108, ALA111, PHE208, CYS323 and ILE325 is left vacant with harmine.

So, the objective was to optimize the β-carboline template for human MAO-A inhibition in order to study this pocket. Previous works carried out on 5*H*-indeno[1,2-*c*]pyridazin-5-ones as MAOs inhibitors have shown it is possible to increase inhibition in this series by substituting the heterocycle core at C(8) by lipophilic and bulky groups like benzyloxy and trifluorobutyloxy.[11,12] Therefore, by structural analogy with 5*H*-indeno[1,2-*c*]pyridazin-5-ones,

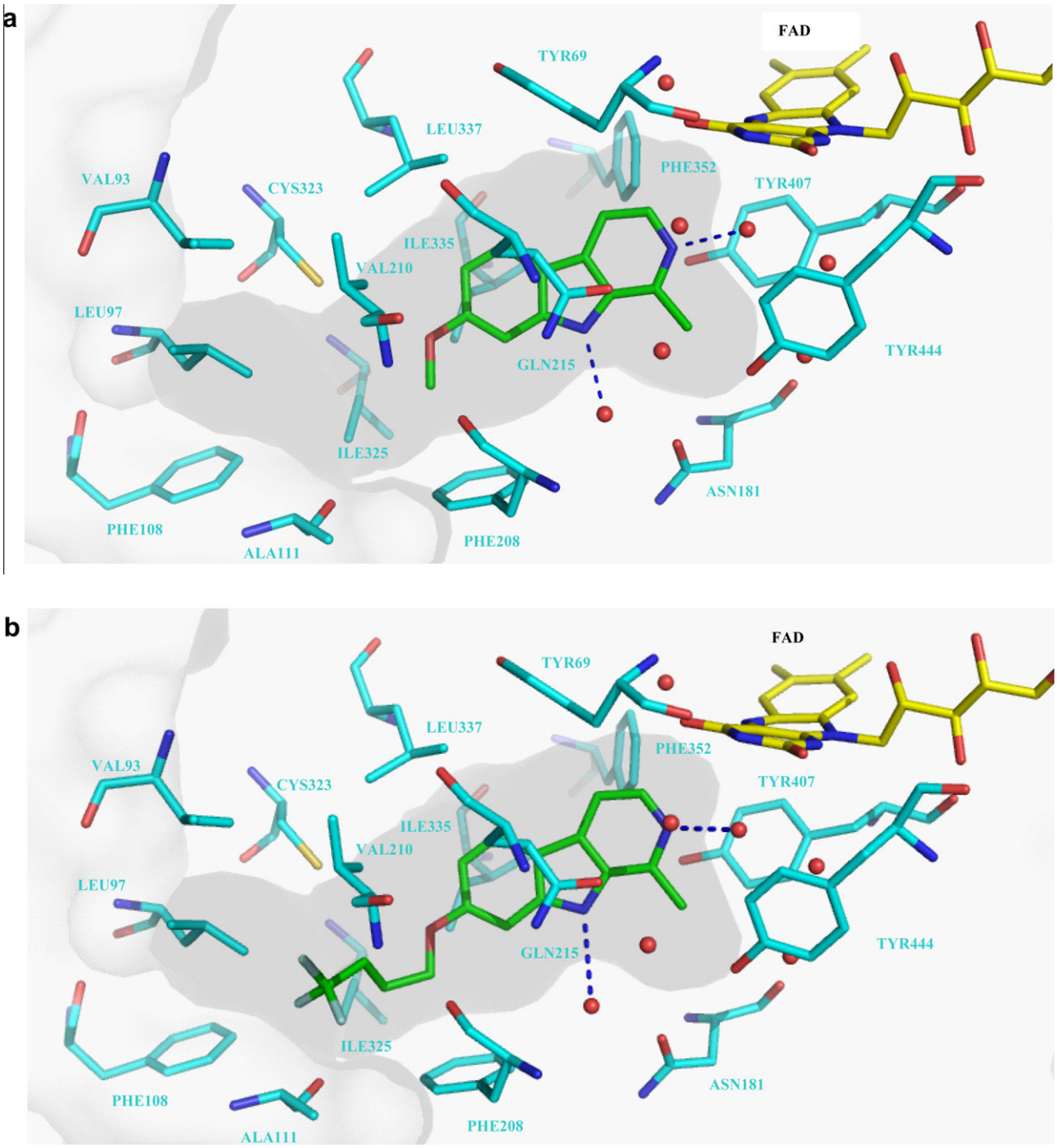

Figure 1. Binding mode of harmine in the cocrystal structure (2Z5X.pdb) (a) and docking solution of compound **3e** (b) in the active site of human MAO-A (2Z5X.pdb). Only amino acids directly implicated in the active site are displayed and labeled in cyan. Harmine and compound **3e** are in green. FAD is in yellow. The water molecules are displayed as red spheres. The hydrogen bonds discussed in the text are depicted as dashed blue lines.

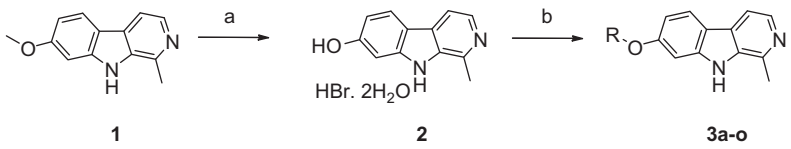

Scheme 1. Synthetic pathway to analogues **3a**–**o**. Reagents and conditions: (a) HBr, HAc, reflux, overnight, yield = 100%; (b) Cs_2CO_3, RX, DMF, room temperature/Δ, yield = 38–92%.

a series of β-carboline derivatives (**3a–o**) substituted at C(7) with lipophilic and bulky groups was synthesized (Scheme 1 and Table 1). All compounds were evaluated for their human MAO-A and MAO-B inhibitory potency and their K_i values were estimated.

2.2. Synthesis of β-carboline analogues

Compounds **3a–o** were synthesized following an original two steps procedure including the demethylation of harmine to the corresponding harmol followed by a re-alkylation of harmol to the corresponding carboline derivative (Scheme 1 and Table 1). The key intermediate, harmol (**2**), was generated by cleavage of the methyl ether present in harmine (**1**) with hydrobromic acid. Finally, compounds **3a–o** were obtained by O-alkylation of harmol in the presence of cesium carbonate with the corresponding alkyl halide.[13] Compounds were characterized by ^{1}H NMR, ^{13}C NMR, mass spectra (MS), melting points (mp), elemental analyses and HPLC.

2.3. Inhibitory potency of harmine and β-carboline analogues against human MAO-A and MAO-B

First, the human MAO-A and MAO-B inhibitory potency of harmine was assayed in vitro against recombinant human MAO isoforms expressed in BTI (*Bacillus thuringiensis israelensis*) insect cells infected with baculovirus. The activity of MAO-A and MAO-B was determined by a luminescent method, according to the procedure developed by Valley et al.[14]

As expected, harmine is a strong and selective MAO-A inhibitor (K_i = 16.9 nM) whereas it poorly inhibits MAO-B (K_i = 120.8 μM) (Fig. 2 and Table 1). This selectivity of harmine for the MAO-A isoenzyme can be explained with the superimposition of the crystal structures of human MAO-A in complex with harmine (2Z5X.pdb) and human MAO-B (2V5Z.pdb)[10,15] (Fig. 3a). The relative geometry of the harmine molecule in human MAO-A could not be accommodated into human MAO-B because of steric overlap with TYR326 of MAO-B. Indeed, the TYR326 side chain in MAO-B produces a restriction that is less pronounced in human MAO-A where ILE335 occupies that position. Thus, ILE335 in MAO-A and TYR326 in MAO-B play a crucial role in inhibitor selectivity in agreement with previous results.[16]

Secondly, the inhibitory potency of the newly synthesized β-carbolines towards human MAO-A and MAO-B was expressed as K_i values (Table 1). All the tested compounds (**3a–o**) present a higher inhibitory potency against MAO-A than MAO-B. The O-alkylation of the compounds by lipophilic groups like aliphatic chains (**3a, b, e**), cyclohexyl (**3f**) and phenyl (**3g, h**) allows to significantly increase the inhibition of MAO-A compared to harmine. The extension of methoxy group by a methoxyethoxy group (**3c**) decreases the inhibition. The substitution of methoxy group of compound (**3c**) by a hydroxyl group (**3d**) does not improve the inhibition. Substitution by a pyridyl group (**3i, j, k**) decreases the inhibition compared to harmine and compound (**3g**). The substitution of phenyl group (**3g**) by a naphthyl group (**3l**) decreases the inhibition. Introduction of more hydrophilic groups like dimethylaminoethyl, dimethylaminopropyl and ethylmorpholine (**3m–o**) highly decreases the inhibition. Compound **3e**, with the trifluorobutyloxy group, is the most active and selective within this series, with a K_i against MAO-A of 3.6 nM (Fig. 2). Moreover, several compounds (**3b**, **e**, **g**, **h**) show a better inhibition on MAO-B (K_i >500 nM) compared to harmine (K_i = 120.8 μM). Interestingly, compound **3f** displayed the best inhibitory activity against MAO-B with a K_i value of 221.6 nM (Fig. 2). This cyclohexyl bearing analogue is also a potent MAO-A inhibitor with a K_i value of 4.3 nM.

Table 1
Structure and inhibitory potency of harmine and the synthesized related β-carbolines against human MAO-A and MAO-B

Compounds	R	K_i[a] (nM)	
		MAO-A	MAO-B
Harmine	$-CH_3$	16.9 (13.7–21.0)	120,800 (94,900–153,900)
3a	$-CH_2CH{=}CH_2$	5.0 (4.5–5.6)	NI[b]
3b	$-CH_2CH(CH_3)_2$	3.9 (2.0–7.7)	>500[c]
3c	$-CH_2CH_2OCH_3$	29.5 (24.0–36.3)	NI
3d	$-CH_2CH_2OH$	28.4 (20.0–40.3)	NI
3e	$-CH_2CH_2CH_2CF_3$	3.6 (2.6–5.0)	>500
3f	$-CH_2C_6H_{11}$	4.3 (3.2–5.6)	221.6 (145.1–338.3)
3g	$-CH_2C_6H_5$	12.6 (11.6–13.7)	>500
3h	$-CH_2CH_2C_6H_5$	5.0 (4.0–6.2)	>500
3i	$-CH_2$-2′-pyridyl	≈500	NI
3j	$-CH_2$-3′-pyridyl	24.9 (20.1–30.7)	NI
3k	$-CH_2$-4′-pyridyl	35.4 (18.9–66.5)	NI
3l	$-CH_2$-2′-naphthyl	100 < K_i < 500	NI
3m	$-CH_2CH_2N(CH_3)_2$	1023.8 (920.0–1139.4)	NI
3n	$-CH_2CH_2CH_2N(CH_3)_2$	684.0 (558.6–836.9)	NI
3o	$-CH_2CH_2$-morpholine	255.7 (196.7–324.5)	NI

[a] Results are expressed as means with in brackets 95% confidence intervals (n = 3).
[b] NI, no inhibition at 1 μM.
[c] >500: inhibition percentage at 1 μM are shown as means with ± SD in brackets (n = 3), **3b** = 14% (±6%), **3e** = 24% (±4%), **3g** = 42% (±2%), **3h** = 39% (±2%).

2.4. X-ray crystal analysis of compound 3e

The molecular structure of compound **3e**, the most active and selective MAO-A inhibitor in our series, was determined by X-ray crystallographic analysis. The compound crystallizes in the trigonal, R_3 space group. Ortep depiction with atom numbering of compound **3e** is shown in Figure 4.

In the molecular structure of **3e**, the planar aromatic β-carboline ring is prolonged by the lateral trifluorobutyloxy chain that adopts a *anti*, *anti*, *gauche*, *anti* conformation [torsion angles are C6–C7–O15–C16 = −176.6(2)°, C7–O15–C16–C17 = 176.6(2)°, O15–C16–C17–C18 = 66.5(3)°, C16–C17–C18–C19 = −174.2(3)°]. The C7–O15–C16 bond angle 117.3(2)° is indicative of a sp^2 character of the oxygen underling electronic delocalization from the β-carboline ring to the alkoxy chain.

Crystal packing results from antiparallel arrangement of molecules. The crystalline cohesion is further maintained by hydrogen bonds formed between N9–H...N2 (2.05 Å), π-hydrogen bonds and weak intermolecular C–H...F hydrogen bonds. So, the crystallographic structure and crystal packing give us information about a

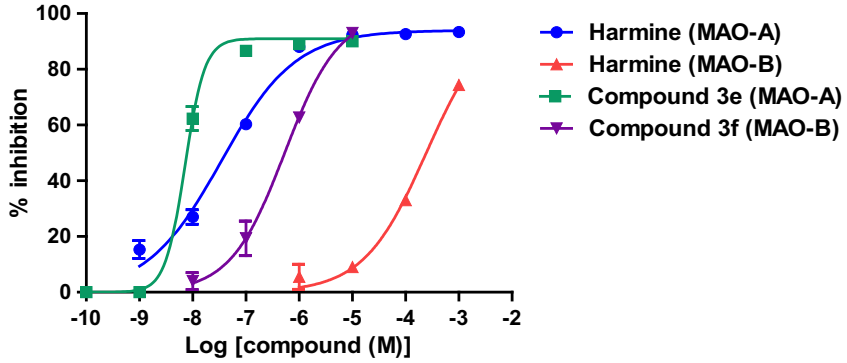

Figure 2. Dose–response curve of harmine on human MAO-A (blue) and on human MAO-B (red), of compound **3e** on human MAO-A (green) and of compound **3f** on human MAO-B (purple). Inhibition percentages are shown as means ± SD with $n = 3$.

low energy conformation which is used as starting point for the docking simulations. Crystal packing further provides insight into types of interactions that compound **3e** can establish within the binding site.

2.5. Molecular docking studies of compound 3e against human MAO-A

Analysis of the optimal binding mode for compound **3e** (Fig. 1b)—identified from the docking study—revealed that this compound is located in the vicinity of the FAD cofactor. The β-carboline derivative incorporates in the active site with harmine-like interactions. In comparison with the harmine interactions, the hydrogen bonds with two water molecules are conserved. The π–π interaction between the amide group of the GLN215 side-chain and harmine is also conserved. The binding mode adopted by compound **3e** allows the trifluorobutyloxy side-chain to settle within a cavity lined with hydrophobic amino acid residues. This hydrophobic pocket includes VAL93, LEU97, PHE108, ALA111, PHE208, VAL210, CYS323 and ILE325. All docking solutions show a similar binding mode but the trifluorobutyl chain is flexible and adopts several conformations. Among these conformations, we selected the *anti, anti, gauche, anti* conformation which also corresponds to the geometry observed in the crystal structure. These data may explain the increase of MAO-A inhibitory potency of compound **3e** ($K_i = 3.6$ nM) compared to harmine ($K_i = 16.9$ nM). Furthermore, the hydrophobic aspect of the cavity around the lateral chain may also explain the increase of inhibition for the compounds with lateral chains displaying lipophilic groups like cyclohexyl (**3f**) or aliphatic chains (**3a, b, e**). The presence of aromatic amino acids in this cavity also allows to favor π–π interactions with phenyl groups (**3g, h**). The fact that the cavity is highly hydrophobic may be one plausible explanation for the decrease in inhibition seen with hydrophilic groups (**3m–o**) compared to harmine.

2.6. Molecular docking studies of compound 3f against human MAO-A and human MAO-B

The interesting result obtained for compound **3f** against human MAO-B led us to study the potential binding mode of this β-carboline derivative with human MAO-A and MAO-B. The results of docking simulations are represented in Figure 3b.

Compound **3f** in MAO-A adopts a similar binding mode compared to derivative **3e** with the cyclohexyl chain pointing to the hydrophobic cavity and stabilization of the β-carboline moiety through two hydrogen bonds and π–π interaction.

Docking simulations against MAO-B were realized with human structure (2V5Z.pdb) in keeping three water molecules conserved in various MAO-B structures which are all buried near the flavine adenine dinucleotide cofactor (FAD).[17] Two water molecules are involved in multiple hydrogen bond networks, while the third one is located in the space defined by the aromatic tyrosine residues (TYR398 and TYR435 which form an 'aromatic cage') and the flavin, and is fixed by the π-systems of the aromatic side chains of TYR398 and TYR435, as well as the central heterocyclic conjugated ring of FAD. In MAO-B, two distinct cavities inside the binding site form an 'entrance cavity' and a 'substrate cavity'.[17] The 'entrance cavity', is connected to the outside of the protein, and the 'substrate cavity', is located in the vicinity of the FAD. These two cavities are separated by ILE199 and TYR326 forming a bottleneck and thus acting as a gate, protecting the catalytic region from the outside. The side chain of ILE199 is the latch that separates the two cavities. It is displayed in Figure 3b as a rotamer in the 'open' position, allowing the β-carboline derivatives to reach both cavities.

Docking simulations for compound **3f** realized against human MAO-B show that the β-carboline core incorporates into the 'substrate cavity' with a shift of the β-carboline orientation compared to docking solution against MAO-A because of steric clash caused by TYR326. Compared to human MAO-A, the β-carboline core is stabilized by only one hydrogen bond between one of the nitrogen atoms of β-carboline and one water molecule. The pyridine function is also stabilized with the aromatic cage (TYR407, TYR444 and FAD) by π–π interaction but the π–π interaction of the β-carboline with the lateral chain of GLN206 is less favorable. This may explain the better inhibitory activity of our compounds against human MAO-A.

In the case of β-carboline derivative **3f**, the lateral chain occupies a hydrophobic pocket of the 'entrance cavity' coated by PHE103, TRP119, LEU164, LEU167, PHE168 and ILE316 where it is stabilized in agreement with an enhanced inhibitory potency towards MAO-B compared to harmine. So, docking simulations allow to explain the stabilization of the cyclohexyl chain in the hydrophobic pocket but also of the aliphatics groups like trifluorobutyl (**3e**) or isobutyl (**3b**). The presence of aromatic amino acids in the hydrophobic pocket allows to understand the inhibition increase for compounds including phenyl groups (**3g** and **h**) compared to harmine. As well as with MAO-A, the fact that the cavity where the lateral chain incorporates is hydrophobic may be related to the absence of inhibition with hydrophilic groups (**3m–o**).

Figure 5a and b shows the schematic diagram of the β-carboline derivatives binding sites against human MAO-A and human MAO-B, respectively. The docking studies against MAO-A and MAO-B have revealed that β-carboline derivatives are located in the vicinity of the FAD cofactor. In both enzymes, the β-carboline core is stabilized by π–π interactions with the aromatic cage (TYR407–TYR444 in MAO-A, TYR398–TYR435 in MAO-B and

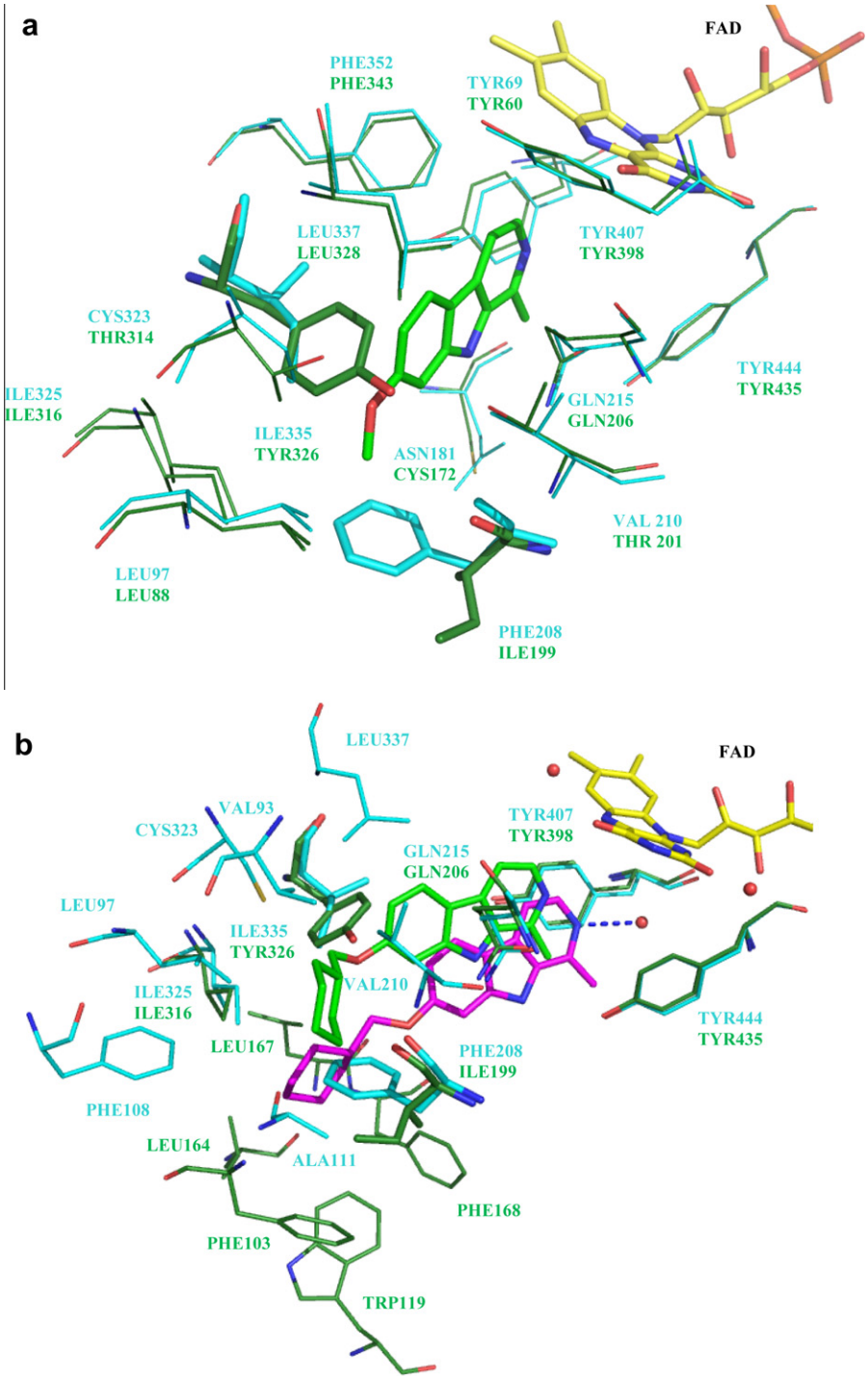

Figure 3. (a) Superimposition of the crystal structures of human MAO-A (cyan, 2Z5X.pdb) in complex with harmine and human MAO-B (green, 2V5Z.pdb). Harmine and FAD are in green and yellow, respectively. (b) Binding mode of compound **3f** in the active site of human MAO-A and human MAO-B. Only amino acids directly implicated in the active site are displayed and labeled in cyan (MAO-A) and in green (MAO-B). Compound **3f** is in green (MAO-A) and magenta (MAO-B). FAD is in yellow. The water molecules involved in MAO-B are displayed as red spheres. The hydrogen bond discussed in the text is depicted as a dashed blue line.

FAD). In contrast to GLN215 in MAO-A, π–π interaction of the β-carboline core with the equivalent amide group of the GLN206 in MAO-B is less favorable. Furthermore, the β-carboline core is stabilized by two hydrogen bonds with water molecules in MAO-A compared to only one hydrogen bond in MAO-B. So, the stabilization of the β-carboline core by the π–π interaction with the amide group of the GLN215 and the two hydrogen bonds may explain the selectivity of the β-carboline derivatives towards MAO-A compared to MAO-B.

In human MAO-A, the lateral chain occupies a hydrophobic pocket including VAL93, LEU97, PHE108, ALA111, PHE208, VAL210, CYS323 and ILE325. The active site of human MAO-A differs from human MAO-B in that it has a monopartite cavity with a total volume of ~550 Å^3.[18] The substrate cavity in human MAO-B has a volume of ~430 Å^3 and that of the entrance cavity is ~290 Å^3. The combined volume of the two cavities when the gating ILE199 is in its open conformation is ~700 Å^3. The TYR326 side chain in MAO-B, although not directly involved in the partition of

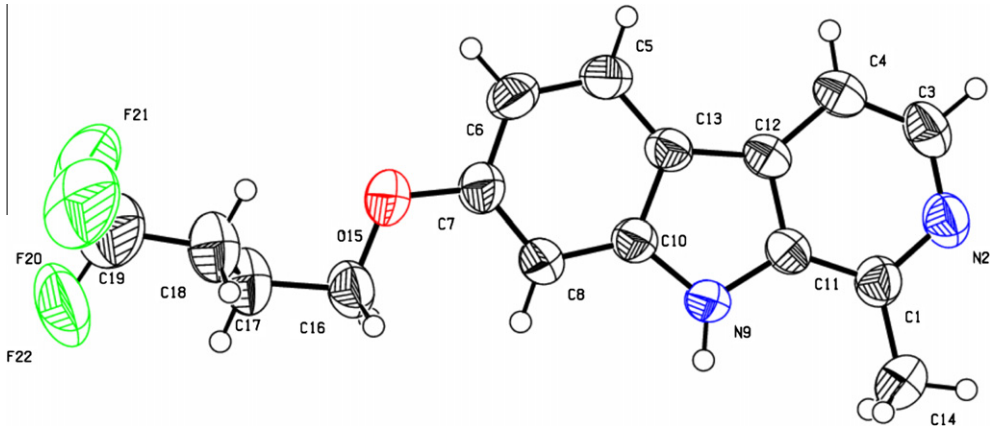

Figure 4. The molecular structure of **3e**, showing the atom-numbering scheme. Displacement ellipsoids are drawn at the 50% probability.

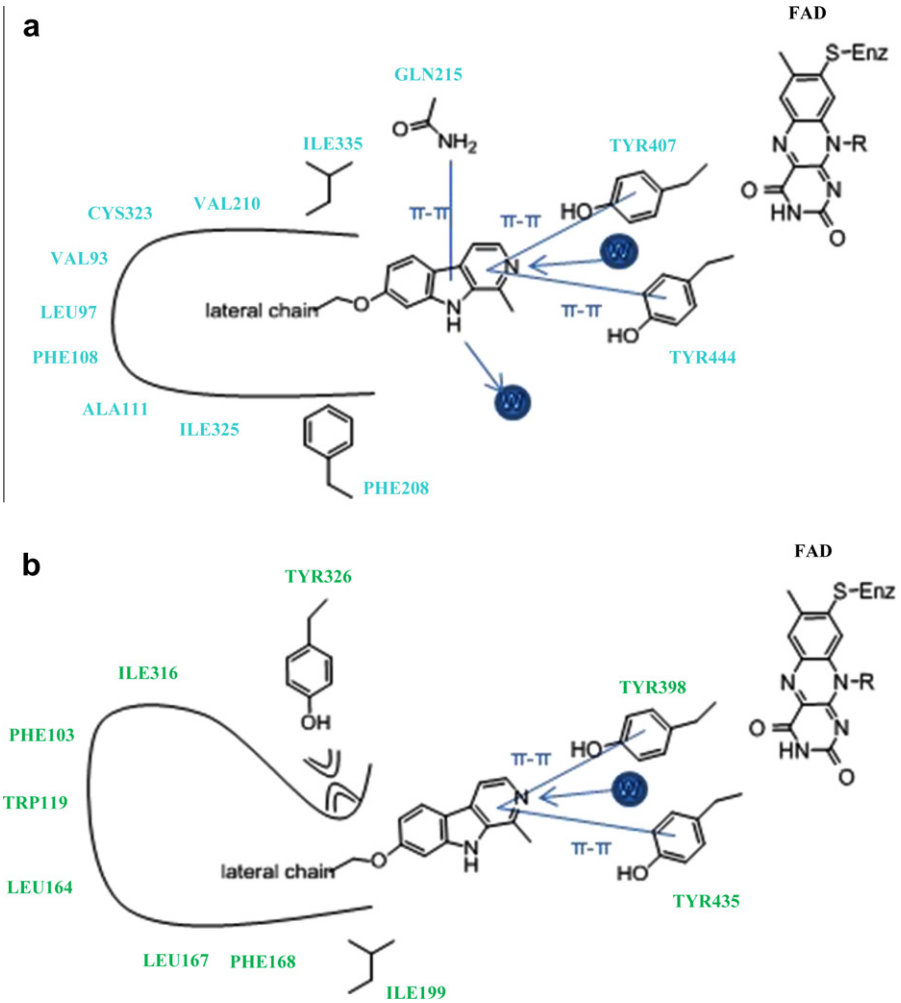

Figure 5. Schematic diagram of the β-carboline derivatives binding sites against human MAO-A (a) and human MAO-B (b). The strongest interactions stabilizing the β-carboline core are represented in blue. The amino acids forming the pocket available for the lateral chain are labeled in cyan (MAO-A) and in green (MAO-B). Hydrogen-bond interactions are represented by a blue line with an arrow head directed towards the electron donor.

the two cavities, does produce a restriction that is less pronounced in human MAO-A where ILE335 occupies that position.[16] Therefore, the MAO-A PHE208–ILE335 and MAO-B ILE199–TYR326 pairs appear to be major determinants in dictating the differential substrate and inhibitor specificities of the two enzymes. In human MAO-B, the lateral chains of studied β-carboline derivatives point to a hydrophobic pocket coated by PHE103, TRP119, LEU164, LEU167, PHE168 and ILE316.

3. Conclusion

In order to design new and more potent MAO-A inhibitors related to harmine, a series of β-carboline analogues has been synthesized. Their inhibitory potency has been evaluated by a luminescent test against human MAO-A and MAO-B enzymes. The results show that the replacement of the methyl moiety of harmine by a lipophilic group like a cyclohexyl, a phenyl or an aliphatic chain increases the inhibition for MAO-A. Compound **3e**, with the trifluorobutyloxy group, is the most active of this series, with a K_i against MAO-A of 3.6 nM. X-ray crystal structure has been determined and gives access to a low energy conformation (*anti, anti, gauche, anti* conformation for the trifluorobutyl chain) which was used as starting point for the docking simulations. Furthermore, the crystal packing provides information about types of interactions that compound **3e** can establish within the binding site. All docking solutions show a similar binding mode of the β-carboline, while the trifluorobutyl chain is flexible. Among conformations of this lateral chain, we retained the conformation of the X-ray crystal structure. Docking simulations into the active site of human MAO-A show that compound **3e** incorporates into the active site with harmine-like interactions. The lateral chain points to the lipophilic pocket where it is stabilized in agreement with an enhanced inhibitory potency towards MAO-A. All the synthesized compounds are selective of MAO-A but some of them show also a moderate MAO-B inhibition (e.g. **3f**, K_i = 221.6 nM) when compared to harmine.

Docking simulations for compound **3f** realized in human MAO-B show that the β-carboline core incorporates into the 'substrate cavity'. A shift is observed for the β-carboline core orientation in MAO-B compared to MAO-A induced by the TYR326 side chain in MAO-B which produces a restriction that is less pronounced in human MAO-A where ILE335 occupies that position. In contrast to GLN215 in MAO-A, π–π interaction of the β-carboline core with the equivalent amide group of the GLN206 in MAO-B is less favorable. In addition, the β-carboline core is stabilized by two hydrogen bonds with water molecules in MAO-A compared to only one hydrogen bond in MAO-B what may explain the selectivity of the β-carboline derivatives towards MAO-A compared to MAO-B. Interestingly, the cyclohexyl chain of compound **3f** points to a lipophilic pocket in the 'entrance cavity' where it is stabilized in agreement with an enhanced inhibitory potency towards MAO-B compared to harmine.

4. Experimental

4.1. Chemicals and instrumentation

^{1}H, ^{13}C and ^{19}F NMR spectra were obtained from a JEOL JNM EX 400 spectrometer (400 MHz for ^{1}H, 100 MHz for ^{13}C and 376 MHz for ^{19}F). The spectra were measured in $CDCl_3$ or DMSO-d_6. NMR spectra are treated with DELTA software. Chemical shifts (δ) are reported in parts per million (ppm) and the coupling constants (J) in Hertz. The following abbreviations are used: s, singlet; d, doublet; t, triplet; m, multiplet; dd, doublet of doublet; dt, doublet of triplet. Melting points were determined with a Totolli–Buchi melting point B-545 apparatus. Analytical thin-layer chromatography (TLC) was performed on Merck silica gel 60 F254 plates. Mass spectra were recorded on an 1100 series MSD Trap spectrometer equipped with an electron spray ionization (ESI) source.

Elemental analyses (C, H, N) were performed on a Thermo Finnigan Flash EA 1112 elemental analyzer. HPLC analyses were realized on a Varian 940-LC apparatus with a Varian 380-LC detector. All the reactions were performed in a two necked round-bottom flask equipped with a septum stopper and an argon-filled balloon. Column chromatographies were performed on silica gel 60 (40–63 μm).

Notes: All chemicals were obtained from Sigma–Aldrich except 4,4,4-trifluoro-1-butanol. 4,4,4-Trifluoro-1-butanol was obtained from Fluorochem Co. For the synthesis of compound **3e**, 4,4,4-trifluoro-1-butanol is first transformed to 1-tosyl-4,4,4-trifluorobutane.[11] To a solution of 4,4,4-trifluoro-1-butanol (2 g, 15.61 mmol) in 20 mL of anhydrous dichloromethane, 2.360 g of triethylamine (23.32 mmol), 2.976 g of *p*-toluenesulfonyl (15.61 mmol) and 0.010 g of 4-(dimethylamino)pyridine (0.082 mmol) are added. The mixture is stirred during 4 h under an inert atmosphere. The crude is washed twice with water and once with hydrochloric acid (HCl 10%). The organic layers are evaporated to dryness under vacuum (0.5 mmHg) to give 3.663 g of the final product (yield = 83%). ^{1}H NMR ($CDCl_3$) δ: 1.89–1.93 (m, 2H, CF_3–CH_2–CH_2), 2.10–2.20 (m, 2H, CF_3–CH_2), 2.45 (s, 3H, Ph–CH_3), 4.08 (t, J = 6.1 Hz, 2H, SO_3–CH_2), 7.35 (d, J = 8.5 Hz, 2H, ArH), 7.78 (d, J = 8.2 Hz, 2H, ArH).

4.2. Synthesis of β-carbolines

4.2.1. Synthesis of harmol hydrobromide dihydrate (2)

Hydrobromic acid 47% aqueous (20 mL) was added to a solution of harmine (1 g, 4.667 mmol) in glacial acetic acid (20 mL). The solution was heated to reflux for 15 h and then allowed to cool to room temperature. The mixture was diluted in water (200 mL), concentrated under reduced pressure and was used without further purification for the following steps. The molecular structure of compound **2** was determined by X-ray crystallographic analysis.

Yield = 100%, R_f = 0.35 (DCM/EtOH 8:2). ^{1}H NMR (DMSO-d_6) δ: 2.92 (s, 3H, CH_3), 6.88 (dd, J_{6-5} = 8.7 Hz, J_{6-8} = 2.1 Hz, 1H, H-6), 6.99 (d, J_{8-6} = 2.1 Hz, 1H, H-8), 8.23 (d, J_{5-6} = 8.7 Hz, 1H, H-5), 8.33 (d, J_{3-4} = 6.4 Hz, 1H, H-3), 8.37 (d, J_{4-3} = 6.2 Hz, 1H, H-4), 10.43 (s, 1H, O–H), 12.45 (s, 1H, N–H). ^{13}C NMR (DMSO-d_6) δ: 16.30 (CH_3), 96.95 (C-8), 113.18 (C_q), 113.31 (C-6), 114.04 (C-4), 125.10 (C-5), 128.96 (C-3), 132.79 (C_q), 133.93 (C_q), 136.78 (C_q), 146.13 (C_q), 161.75 (C_q). MS: $[M+H]^+$ 199.1, mp 247.9 °C.

4.2.2. General procedure for the synthesis of 7-alkoxy-1-methyl-β-carbolines (3a–o)

The 7-alkoxy-1-methyl-β-carbolines (**3a–o**) were synthesized according to a previously reported procedure.[13] The appropriate alkyl halide (by portion) or 1-tosyl-4,4,4-trifluorobutane (for compound **3e**) and cesium carbonate were added to harmol (**2**) dissolved in anhydrous dimethylformamide (DMF). Then, the reaction mixture was stirred at room temperature or heated for several hours. At the end of the reaction, the mixture was cooled and diluted with dichloromethane, washed once with water and three times with brine. The organic layer was dried over $MgSO_4$ and concentrated. The crude product was purified by liquid chromatography.

4.2.2.1. 7-(Allyloxy)-1-methyl-β-carboline (3a). Compound **3a** was obtained from a solution of harmol (0.250 g, 0.796 mmol), cesium carbonate (0.804 g, 2.468 mmol) and 3-bromo-1-propene (0.119 g, 0.982 mmol) in 5 mL of DMF. The reaction mixture was stirred at room temperature for 24 h. The crude product was purified by column chromatography (dichloromethane/ethanol 95:5% v/v).

Yield 75%, R_f = 0.63 (DCM/EtOH 8:2). ^{1}H NMR ($CDCl_3$) δ: 2.79 (s, 3H, CH_3), 4.63 (dt, J = 1.4 Hz, J = 5.3 Hz, 2H, O–CH_2), 5.30–5.34 (m, 1H, O–CH_2CH=CH_2), 5.43–5.48 (m, 1H, O–CH_2CH=CH_2), 6.05–6.15 (m, 1H, O–CH_2CH), 6.92 (dd, J_{6-5} = 8.7 Hz, J_{6-8} = 2.3 Hz, 1H, H-6), 6.97 (d, J_{8-6} = 2.1 Hz, 1H, H-8), 7.71 (d, J_{4-3} = 5.5 Hz, 1H, H-4), 7.96 (d, J_{5-6} = 8.7 Hz, 1H, H-5), 8.31 (d, J_{3-4} = 5.5 Hz, 1H, H-3), 8.39 (s, 1H, N–H). ^{13}C NMR ($CDCl_3$) δ: 20.23 (CH_3), 69.31 (O–CH_2), 95.93 (C-8), 110.34 (C-6), 112.36 (C-4), 116.05 (C_q), 118.05 (O–CH_2CH=CH_2), 122.79 (C-5), 128.77 (C_q), 133.14 (O–CH_2CH),

134.72 (C_q), 138.81 (C-3), 141.00 (C_q), 141.72 (C_q), 159.87 (C_q). MS: $[M+H]^+$ 239.1. Anal. Calcd for $C_{15}H_{14}N_2O + ½H_2O$: C, 72.85%; H, 6.11%; N, 11.33%. Found: C, 73.76%; H, 5.82%; N, 11.14%. Purity by HPLC: 99%, mp 173.9 °C.

4.2.2.2. 7-(Isobutyloxy)-1-methyl-β-carboline (3b). Compound **3b** was obtained from a solution of harmol (0.307 g, 0.978 mmol), cesium carbonate (1.764 g, 5.414 mmol) and 1-bromo-2-methylpropane (0.283 g, 2.065 mmol) in 6 mL of DMF. The reaction mixture was heated at 60 °C for 24 h. The crude product was purified by column chromatography (dichloromethane/ethanol 95:5% v/v).

Yield 87%, R_f = 0.65 (DCM/EtOH 8:2). ^{1}H NMR ($CDCl_3$) δ: 1.02 (d, J = 6.9 Hz, 6H, CH–(CH_3)$_2$), 2.05–2.15 (m, 1H, CH–(CH_3)$_2$), 2.78 (s, 3H, CH_3), 3.74 (d, J = 6.4 Hz, 2H, O–CH_2), 6.88–6.90 (m, 2H, H-8 + H-6), 7.74 (d, J_{4-3} = 5.3 Hz, 1H, H-4), 7.95 (d, J_{5-6} = 9.4 Hz, 1H, H-5), 8.34 (d, J_{3-4} = 5.3 Hz, 1H, H-3), 10.05 (s, 1H, N–H). ^{13}C NMR ($CDCl_3$) δ: 19.39 (CH–(CH_3)$_2$), 20.25 (CH_3), 28.40 (CH–(CH_3)$_2$), 74.87 (O–CH_2), 95.51 (C-8), 110.26 (C-6), 112.37 (C-4), 115.65 (C_q), 122.65 (C-5), 128.86 (C_q), 134.93 (C_q), 138.47 (C-3), 141.09 (C_q), 142.15 (C_q), 160.58 (C_q). MS: $[M+H]^+$ 255.1. Anal. Calcd for $C_{16}H_{18}N_2O$: C, 75.56%; H, 7.13%; N, 11.01%. Found: C, 75.54%; H, 7.19%; N, 10.75%. Purity by HPLC: 98%, mp 202.9 °C.

4.2.2.3. 7-(2-Methoxyethoxy)-1-methyl-β-carboline (3c). Compound **3c** was obtained from a solution of harmol (0.258 g, 0.822 mmol), cesium carbonate (1.135 g, 3.484 mmol) and 2-chloroethyl methyl ether (0.140 g, 1.481 mmol) in 5 mL of DMF. The reaction mixture was heated at 60 °C for 24 h. The crude product was purified by column chromatography (dichloromethane/ethanol 95:5% v/v).

Yield 70%, R_f = 0.55 (DCM/EtOH 8:2). ^{1}H NMR ($CDCl_3$) δ: 2.82 (s, 3H, CH_3), 3.45 (s, 3H, O–CH_3), 3.76 (t, J = 4.6 Hz, 2H, CH_2), 4.15 (t, J = 4.6 Hz, 2H, CH_2), 6.91 (dd, J_{6-8} = 1.8 Hz, J_{6-5} = 8.7 Hz, 1H, H-6), 7.00 (d, J_{8-6} = 1.4 Hz, 1H, H-8), 7.73 (d, J_{4-3} = 5.5 Hz, 1H, H-4), 7.93 (d, J_{5-6} = 8.7 Hz, 1H, H-5), 8.26 (d, J_{3-4} = 5.3 Hz, 1H, H-3), 9.78 (s, 1H, N–H). ^{13}C NMR ($CDCl_3$) δ: 19.66 (CH_3), 59.34 (O–CH_3), 67.72 (–CH_2–), 71.06 (–CH_2–), 95.75 (C-8), 110.68 (C-6), 112.54 (C-4), 115.72 (C_q), 122.80 (C-5), 129.32 (C_q), 134.88 (C_q), 137.00 (C-3), 140.56 (C_q), 142.59 (C_q), 160.37 (C_q). MS: $[M+H]^+$ 257.1. Anal. Calcd for $C_{15}H_{16}N_2O_2 + ½H_2O$: C, 67.91%; H, 6.46%; N, 10.56%. Found: C, 67.85%; H, 6.31%; N, 10.48%. Purity by HPLC: 99%, mp 175.8 °C.

4.2.2.4. 7-(2-Hydroxyethyloxy)-1-methyl-β-carboline (3d). Compound **3d** was obtained from a solution of harmol (0.845 g, 2.691 mmol), cesium carbonate (3.070 g, 9.422 mmol) and 2-chloroethanol (0.600 g, 7.459 mmol) in 8 mL of DMF. The reaction mixture was refluxed for 15 h. The crude product was purified by column chromatography (toluene/ethanol 80: 20% v/v).

Yield 58%, R_f = 0.33 (DCM/EtOH 8:2). ^{1}H NMR (DMSO-d_6) δ: 2.68 (s, 3H, CH_3), 3.75 (dt, J = 4.6 Hz, J = 5.1 Hz, 2H, CH_2–OH), 4.06 (t, J = 4.6 Hz, 2H, O–CH_2), 4.89 (t, J = 5.1 Hz, 1H, CH_2–OH), 6.81 (dd, J_{6-5} = 8.7 Hz, J_{6-8} = 2.1 Hz, 1H, H-6), 6.97 (d, J_{8-6} = 2.1 Hz, 1H, H-8), 7.77 (d, J_{4-3} = 5.3 Hz, 1H, H-4), 8.01 (d, J_{5-6} = 8.7 Hz, 1H, H-5), 8.11 (d, J_{3-4} = 5.3 Hz, 1H, H-3), 11.37 (s, 1H, N–H). ^{13}C NMR (DMSO-d_6) δ: 18.16 (CH_3), 60.06 (CH_2–OH), 70.58 (O–CH_2), 95.62 (C-8), 112.01 (C-6), 113.78 (C-4), 114.64 (C_q), 124.42 (C-5), 130.81 (C_q), 132.81 (C-3), 134.56 (C_q), 139.32 (C_q), 144.57 (C_q), 161.69 (C_q). MS: $[M+H]^+$ 243.0. Anal. Calcd for $C_{14}H_{14}N_2O_2$: C, 69.41%; H, 5.82%; N, 11.56%. Found: C, 68.70%; H, 5.59%; N, 10.77%. Purity by HPLC: 97%, mp 264.4 °C.

4.2.2.5. 7-(4,4,4-Trifluorobutoxy)-1-methyl-β-carboline (3e). Compound **3e** was obtained from a solution of harmol (0.100 g, 0.318 mmol), cesium carbonate (0.330 g, 1.013 mmol) and 1-tosyl-4,4,4-trifluorobutane (0.150 g, 0.531 mmol) in 7 mL of DMF. The reaction mixture was heated at 90 °C for 7 h. The crude product was purified by column chromatography (dichloromethane/ethanol 90:10% v/v).

Yield 72%, R_f = 0.67 (DCM/EtOH 8:2). ^{1}H NMR (DMSO-d_6) δ: 1.94–2.01 (m, 2H, CF_3–CH_2–CH_2), 2.39–2.52 (m, 2H, CF_3–CH_2, overlap with DMSO), 2.68 (s, 3H, CH_3), 4.12 (t, J = 6.2 Hz, 2H, O–CH_2), 6.82 (dd, J_{6-5} = 8.7 Hz, J_{6-8} = 2.1 Hz, 1H, H-6), 6.97 (d, J_{8-6} = 2.1 Hz, 1H, H-8), 7.77 (d, J_{4-3} = 5.3 Hz, 1H, H-4), 8.02 (d, J_{5-6} = 8.7 Hz, 1H, H-5), 8.11 (d, J_{3-4} = 5.3 Hz, 1H, H-3), 11.38 (s, 1H, N–H). ^{13}C NMR (DMSO-d_6) δ: 20.88 (CH_3), 22.25 (d, J = 2.9 Hz, CF_3–CH_2–CH_2), 30.13 (q, J = 27.8 Hz, CF_3–CH_2), 66.55 (O–CH_2), 95.88 (C-8), 109.85 (C-6), 112.49 (C-4), 115.56 (C_q), 123.21 (C-5), 127.69 (C_q), 135.06 (C_q), 138.29 (C-3), 141.83 (C_q), 142.36 (C_q), 159.59 (C_q). ^{19}F NMR (DMSO-d_6) δ: −64.67 (t, J = 11.5 Hz). MS: $[M+H]^+$ 309.1. Anal. Calcd for $C_{16}H_{15}F_3N_2O$: C, 62.33%; H, 4.90%; N, 9.09%. Found: C, 62.68%; H, 4.75%; N, 9.09%. Purity by HPLC: 98%, mp 284.3 °C.

4.2.2.6. 7-(Cyclohexylmethoxy)-1-methyl-β-carboline (3f). Compound **3f** was obtained from a solution of harmol (0.200 g, 0.637 mmol), cesium carbonate (0.911 g, 2.796 mmol) and (bromomethyl)cyclohexane (0.286 g, 1.615 mmol) in 5 mL of DMF. The reaction mixture was stirred at room temperature for 30 h. The crude product was purified by column chromatography (dichloromethane/ethanol 95:5% v/v).

Yield 85%, R_f = 0.65 (DCM/EtOH 8:2). ^{1}H NMR ($CDCl_3$) δ: 1.03–1.37 (m, 5H, CH (cyclohexyl)), 1.70–1.92 (m, 6H, CH (cyclohexyl)), 2.79 (s, 3H, CH_3), 3.84 (d, J = 6.2 Hz, 2H, O–CH_2), 6.89 (dd, J_{6-8} = 2.1 Hz, J_{6-5} = 8.7 Hz, 1H, H-6), 6.93 (d, J_{8-6} = 2.1 Hz, 1H, H-8), 7.70 (d, J_{4-3} = 5.3 Hz, 1H, H-4), 7.94 (d, J_{5-6} = 8.7 Hz, 1H, H-5), 8.19 (s, 1H, N–H), 8.31 (d, J_{3-4} = 5.5 Hz, 1H, H-3). ^{13}C NMR ($CDCl_3$) δ: 20.36 (CH_3), 25.91 (CH (cyclohexyl)), 26.61 (CH (cyclohexyl)), 30.04 (CH (cyclohexyl)), 37.79 (CH (cyclohexyl)), 73.99 (O–CH_2), 95.44 (C-8), 110.29 (C-6), 112.27 (C-4), 115.72 (C_q), 122.68 (C-5), 128.73 (C_q), 134.63 (C_q), 139.12 (C-3), 140.98 (C_q), 141.67 (C_q), 160.61 (C_q). MS: $[M+H]^+$ 295.2. Anal. Calcd for $C_{19}H_{22}N_2O$: C, 77.52%; H, 7.53%; N, 9.52%. Found: C, 76.59%; H, 7.03%; N, 8.87%. Purity by HPLC: 97%, mp 231.8 °C.

4.2.2.7. 7-(Benzyloxy)-1-methyl-β-carboline (3g). Compound **3g** was obtained from a solution of harmol (0.500 g, 1.592 mmol), cesium carbonate (1.410 g, 4.328 mmol) and 1-bromomethylbenzene (0.432 g, 2.526 mmol) in 10 mL of DMF. The reaction mixture was stirred at room temperature for 5 h. The crude product was purified by column chromatography (dichloromethane/ethanol 95:5% v/v).

Yield 70%, R_f = 0.69 (DCM/EtOH 8:2). ^{1}H NMR ($CDCl_3$) δ: 2.78 (s, 3H, CH_3), 5.17 (s, 2H, O–CH_2), 6.98 (dd, J_{6-5} = 8.7 Hz, J_{6-8} = 2.3 Hz, 1H, H-6), 7.01 (d, J_{8-6} = 2.1 Hz, 1H, H-8), 7.32–7.47 (m, 5H, ArH), 7.71 (d, J_{4-3} = 5.5 Hz, 1H, H-4), 7.97 (d, J_{5-6} = 8.5 Hz, 1H, H-5), 8.28 (s, 1H, N–H), 8.32 (d, J_{3-4} = 5.3 Hz, 1H, H-3). ^{13}C NMR ($CDCl_3$) δ: 20.31 (CH_3), 70.50 (O–CH_2), 96.11 (C-8), 110.39 (C-6), 112.34 (C-4), 116.16 (C_q), 122.82 (C-5), 127.56 (C–ArH), 128.18 (C–ArH), 128.64 (C_q), 128.77 (C–ArH), 134.74 (C_q), 136.84 (C_q), 139.06 (C-3), 141.12 (C_q), 141.60 (C_q), 159.96 (C_q). MS: $[M+H]^+$ 289.1. Anal. Calcd for $C_{19}H_{16}N_2O$: C, 79.14%; H, 5.59%; N, 9.72%. Found: C, 78.99%; H, 5.60%; N, 9.60%. Purity by HPLC: 99%, mp 212.3 °C.

4.2.2.8. 7-(Phenethoxy)-1-methyl-β-carboline (3h). Compound **3h** was obtained from a solution of harmol (0.280 g, 0.892 mmol), cesium carbonate (3.010 g, 9.238 mmol) and (2-chloroethyl)benzene (0.363 g, 2.582 mmol) in 5 mL of DMF. The reaction mixture was refluxed for 30 h. The crude product was purified by column chromatography (dichloromethane/ethanol 95:5% v/v).

Yield 72%, R_f = 0.67 (DCM/EtOH 8:2). ^{1}H NMR ($CDCl_3$) δ: 2.78 (s, 3H, CH_3), 3.14 (t, J = 7.1 Hz, 2H, O–CH_2–CH_2), 4.24 (t, J = 7.1 Hz, 2H,

O–CH_2), 6.89 (dd, 1H, J_{6-5} = 8.7 Hz, J_{6-8} = 2.3 Hz, H-6), 6.93 (d, J_{8-6} = 2.1 Hz, 1H, H-8), 7.22–7.34 (m, 5H, ArH), 7.71 (d, J_{4-3} = 5.3 Hz, 1H, H-4), 7.94 (d, J_{5-6} = 8.5 Hz, 1H, H-5), 8.30 (d, J_{3-4} = 5.5 Hz, 1H, H-3), 8.89 (s, 1H, N–H). ^{13}C NMR ($CDCl_3$) δ: 20.16 (CH_3), 35.85 (CH_2), 69.16 (O–CH_2), 95.64 (C-8), 110.27 (C-6), 112.37 (C-4), 115.89 (C_q), 122.78 (C-5), 126.68 (C–ArH), 128.63 (C–ArH), 128.84 (C_q), 129.12 (C–ArH), 134.80 (C_q), 138.20 (C_q), 138.52 (C-3), 140.98 (C_q), 141.94 (C_q), 160.12 (C_q). MS: $[M+H]^+$ 303.1. Anal. Calcd for $C_{20}H_{18}N_2O$: C, 79.44%; H, 6.00%; N, 9.26%. Found: C, 78.33%; H, 5.94%; N, 8.88%. Purity by HPLC: 99%, mp 139.7 °C.

4.2.2.9. 7-(Pyridin-2-ylmethoxy)-1-methyl-β-carboline (3i). Compound **3i** was obtained from a solution of harmol (0.362 g, 1.153 mmol), cesium carbonate (1.771 g, 5.436 mmol) and 2-(bromomethyl)pyridine hydrobromide (0.363 g, 1.435 mmol) in 7 mL of DMF. The reaction mixture was stirred at room temperature for 24 h. The crude product was purified by column chromatography (dichloromethane/ethanol 90:10% v/v).

Yield 90%, R_f = 0.56 (DCM/EtOH 8:2). ^{1}H NMR ($CDCl_3$) δ: 2.76 (s, 3H, CH_3), 5.29 (s, 2H, O–CH_2), 6.97–7.00 (m, 2H, H-6 + H-8), 7.23 (dd, J = 5.5 Hz, J = 7.1 Hz, 1H, ArH), 7.55 (d, J = 8.0 Hz, 1H, ArH), 7.69–7.73 (m, 2H, H-4 + ArH), 7.97 (d, J_{5-6} = 9.2 Hz, 1H, H-5), 8.31 (d, J_{3-4} = 5.5 Hz, 1H, H-3), 8.59 (d, J = 4.8 Hz, 1H, ArH), 8.94 (s, 1H, N–H). ^{13}C NMR ($CDCl_3$) δ: 20.33 (CH_3), 71.01 (O–CH_2), 96.01 (C-8), 110.36 (C-6), 112.36 (C-4), 116.26 (C_q), 121.56 (C–ArH), 122.87 (C–ArH), 122.90 (C-5), 128.58 (C_q), 134.88 (C_q), 137.09 (C–ArH), 138.83 (C-3), 141.24 (C_q), 141.74 (C_q), 149.29 (C–ArH), 157.12 (C_q), 159.46 (C_q). MS: $[M+H]^+$ 290.1. Anal. Calcd for $C_{18}H_{15}N_3O$: C, 74.72%; H, 5.23%; N, 14.52%. Found: C, 74.23%; H, 5.23%; N, 14.22%. Purity by HPLC: 99%, mp 187.5 °C.

4.2.2.10. 7-(Pyridin-3-ylmethoxy)-1-methyl-β-carboline (3j). Compound **3j** was obtained from a solution of harmol (0.355 g, 1.131 mmol), cesium carbonate (1.550 g, 4.757 mmol) and 3-(bromomethyl)pyridine hydrobromide (0.342 g, 1.352 mmol) in 7 mL of DMF. The reaction mixture was stirred at room temperature for 24 h. The crude product was purified by column chromatography (dichloromethane/ethanol 90:10% v/v).

Yield 91%, R_f = 0.44 (DCM/EtOH 8:2). ^{1}H NMR ($CDCl_3$) δ: 2.78 (s, 3H, CH_3), 5.15 (s, 2H, O–CH_2), 6.96 (dd, J_{6-5} = 8.7 Hz, J_{6-8} = 2.1 Hz, 1H, H-6), 6.99 (d, J_{8-6} = 2.1 Hz, 1H, H-8), 7.33 (dd, J = 4.8 Hz, J = 7.8 Hz, 1H, ArH), 7.73 (d, 1H, J_{4-3} = 5.5 Hz, 1H, H-4), 7.80 (dt, J = 1.8 Hz, J = 8.0 Hz, 1H, ArH), 7.99 (d, J_{5-6} = 8.7 Hz, 1H, H-5), 8.32 (d, J_{3-4} = 5.3 Hz, 1H, H-3), 8.59 (dd, J = 1.4 Hz, J = 4.6 Hz, 1H, ArH), 8.71 (d, J = 1.6 Hz, 1H, ArH), 9.22 (s, 1H, N–H). ^{13}C NMR ($CDCl_3$) δ: 20.29 (CH_3), 68.00 (O–CH_2), 96.25 (C-8), 110.08 (C-6), 112.41 (C-4), 116.47 (C_q), 122.96 (C-5), 123.74 (C–ArH), 128.61 (C_q), 132.53 (C_q), 134.96 (C_q), 135.49 (C–ArH), 138.78 (C-3), 141.28 (C_q), 141.81 (C_q), 149.02 (C–ArH), 149.56 (C–ArH), 159.47 (C_q). MS: $[M+H]^+$ 290.1. Anal. Calcd for $C_{18}H_{15}N_3O$ + ½H_2O: C, 72.47%; H, 5.41%; N, 14.08%. Found: C, 72.66%; H, 5.32%; N, 14.01%. Purity by HPLC: 99%, mp 226.6 °C.

4.2.2.11. 7-(Pyridin-4-ylmethoxy)-1-methyl-β-carboline (3k). Compound **3k** was obtained from a solution of harmol (0.355 g, 1.131 mmol), cesium carbonate (1.695 g, 5.202 mmol) and 4-(bromomethyl)pyridine hydrobromide (0.378 g, 1.494 mmol) in 7 mL of DMF. The reaction mixture was stirred at room temperature for 24 h. The crude product was purified by column chromatography (dichloromethane/ethanol 90:10% v/v).

Yield 62%, R_f = 0.39 (DCM/EtOH 8:2). ^{1}H NMR ($CDCl_3$) δ: 2.77 (s, 3H, CH_3), 5.20 (s, 2H, O–CH_2), 6.95–6.99 (m, 2H, H-6 + H-8), 7.39 (d, J = 5.5 Hz, 2H, ArH), 7.72 (d, J_{4-3} = 5.3 Hz, 1H, H-4), 8.00 (d, J_{5-6} = 9.2 Hz, 1H, H-5), 8.32 (d, J_{3-4} = 5.5 Hz, 1H, H-3), 8.48 (s, 1H, N–H), 8.62 (d, J = 5.7 Hz, 2H, ArH). ^{13}C NMR ($CDCl_3$) δ: 20.34 (CH_3), 68.65 (O–CH_2), 96.21 (C-8), 110.05 (C-6), 112.39 (C-4), 116.60 (C_q), 121.58 (C–ArH), 123.04 (C-5), 128.49 (C_q), 134.82 (C_q), 139.16 (C-3), 141.28 (C_q), 141.51 (C_q), 146.19 (C_q), 150.14 (C–ArH), 159.24 (C_q). MS: $[M+H]^+$ 290.1. Anal. Calcd for $C_{18}H_{15}N_3O$ + ½H_2O: C, 72.47%; H, 5.41%; N, 14.08%. Found: C, 72.05%; H, 5.34%; N, 14.11%. Purity by HPLC: 99%, mp 232.5 °C.

4.2.2.12. 7-(Naphthalen-2-ylmethoxy)-1-methyl-β-carboline (3l). Compound **3l** was obtained from a solution of harmol (0.500 g, 1.592 mmol), cesium carbonate (1.555 g, 4.773 mmol) and 2-(bromomethyl)naphthalene (0.540 g, 2.442 mmol) in 10 mL of DMF. The reaction mixture was stirred at room temperature for 6 h. The crude product was purified by column chromatography (dichloromethane/ethanol 95:5% v/v).

Yield 82%, R_f = 0.70 (DCM/EtOH 8:2). ^{1}H NMR (DMSO-d_6) δ: 2.67 (s, 3H, CH_3), 5.38 (s, 2H, O–CH_2), 6.94 (dd, J_{6-8} = 2.1 Hz, J_{6-5} = 8.5 Hz, 1H, H-6), 7.09 (d, J_{8-6} = 2.3 Hz, 1H, H-8), 7.47–7.53 (m, 2H, ArH), 7.61 (dd, J = 1.6 Hz, J = 8.5 Hz, 1H, ArH), 7.77 (d, J_{4-3} = 5.3 Hz, 1H, H-4), 7.89–7.95 (m, 3H, ArH), 8.01 (s, 1H, ArH), 8.04 (d, J_{5-6} = 8.7 Hz, 1H, H-5), 8.11 (d, J_{3-4} = 5.3 Hz, 1H, H-3), 11.38 (s, 1H, N–H). ^{13}C NMR (DMSO-d_6) δ: 20.86 (CH_3), 70.19 (O–CH_2), 96.49 (C-8), 110.24 (C-6), 112.49 (C-4), 115.61 (C_q), 123.22 (C-5), 126.18 (C–ArH), 126.68 (C–ArH), 126.72 (C–ArH), 126.90 (C–ArH), 127.67 (C_q), 128.17 (C–ArH), 128.33 (C–ArH), 128.66 (C–ArH), 133.09 (C_q), 133.35 (C_q), 135.10 (C_q), 135.33 (C_q), 138.29 (C-3), 141.85 (C_q), 142.30 (C_q), 159.60 (C_q). MS: $[M+H]^+$ 339.2. Anal. Calcd for $C_{23}H_{18}N_2O$: C, 81.63%; H, 5.36%; N, 8.28%. Found: C, 81.50%; H, 5.29%; N, 7.99%. Purity by HPLC: 99%, mp 238.6 °C.

4.2.3. 7-(*N*,*N*-Dimethylaminoethyloxy)-1-methyl-β-carboline (3m)

Compound **3m** was obtained from a solution of harmol (0.440 g, 1.401 mmol), cesium carbonate (2.060 g, 6.322 mmol) and 2-chloro-*N*,*N*-dimethylethylamine hydrochloride (0.330 g, 2.291 mmol) in 10 mL of DMF. The reaction mixture was heated at 110 °C for 7 h. The crude product was purified by column chromatography (dichloromethane/ethanol/triethylamine 80:20:2% v/v/v).

Yield 44%, R_f = 0.26 (DCM/EtOH/NEt_3 8:2:0.2). ^{1}H NMR ($CDCl_3$) δ: 2.35 (s, 6H, 2CH_3), 2.77 (t, J = 5.7 Hz, 2H, O–CH_2–CH_2), 2.78 (s, 3H, CH_3), 4.12 (t, J = 5.7 Hz, 2H, O–CH_2), 6.90 (dd, J_{6-5} = 8.5 Hz, J_{6-8} = 2.1 Hz, 1H, H-6), 6.94 (d, J_{8-6} = 2.1 Hz, 1H, H-8), 7.71 (d, J_{4-3} = 5.5 Hz, 1H, H-4), 7.94 (d, J_{5-6} = 8.7 Hz, 1H, H-5), 8.31 (d, J_{3-4} = 5.3 Hz, 1H, H-3), 8.94 (s, 1H, N–H). ^{13}C NMR ($CDCl_3$) δ: 20.34 (CH_3), 46.06 (2CH_3), 58.39 (O–CH_2–CH_2), 66.43 (O–CH_2), 95.65 (C-8), 110.11 (C-6), 112.34 (C-4), 115.96 (C_q), 122.69 (C-5), 128.69 (C_q), 134.87 (C_q), 138.79 (C-3), 141.16 (C_q), 141.85 (C_q), 160.05 (C_q). MS: $[M+H]^+$ 270.1. Anal. Calcd for $C_{16}H_{19}N_3O$ + ½H_2O: C, 69.04%; H, 7.24%; N, 15.10%. Found: C, 68.95%; H, 6.79%; N, 14.50%. Purity by HPLC: 99%, mp 218.3 °C.

4.2.4. 7-(*N*,*N*-Dimethylaminopropyloxy)-1-methyl-β-carboline (3n)

Compound **3n** was obtained from a solution of harmol (0.400 g, 1.274 mmol), cesium carbonate (1.450 g, 4.450 mmol) and 3-chloro-*N*,*N*-dimethylpropylamine hydrochloride (0.440 g, 2.784 mmol) in 10 mL of DMF. The reaction mixture was heated at 110 °C for 7 h. The crude product was purified by column chromatography (dichloromethane/ethanol/triethylamine 80:20:2% v/v/v).

Yield 52%, R_f = 0.22 (DCM/EtOH/NEt_3 8:2:0.2). ^{1}H NMR ($CDCl_3$) δ: 2.00–2.07 (m, 2H, O–CH_2–CH_2), 2.30 (s, 6H, 2CH_3), 2.53 (t, J = 7.2 Hz, 2H, O–CH_2–CH_2–CH_2), 2.79 (s, 3H, CH_3), 4.12 (t, J = 6.4 Hz, 2H, O–CH_2), 6.89 (dd, J_{6-5} = 8.6 Hz, J_{6-8} = 2.1 Hz, 1H, H-6), 6.96 (d, J_{8-6} = 2.0 Hz, 1H, H-8), 7.70 (d, J_{4-3} = 5.5 Hz, 1H, H-4), 7.94 (d, J_{5-6} = 8.7 Hz, 1H, H-5), 8.12 (s, 1H, N–H), 8.31 (d, J_{3-4} = 5.3 Hz, 1H,

H-3). ^{13}C NMR ($CDCl_3$) δ: 20.38 (CH_3), 27.59 (O–CH_2–CH_2), 45.65 ($2CH_3$), 56.52 (O–CH_2–CH_2–CH_2), 66.54 (O–CH_2), 95.54 (C-8), 109.91 (C-6), 112.39 (C-4), 115.71 (C_q), 122.60 (C-5), 128.76 (C_q), 135.23 (C_q), 138.23 (C-3), 141.32 (C_q), 142.37 (C_q), 160.17 (C_q). MS: $[M+H]^+$ 284.1. Anal. Calcd for $C_{17}H_{21}N_3O + ½H_2O$: C, 69.84%; H, 7.58%; N, 14.37%. Found: C, 69.82%; H, 7.42%; N, 14.06%. Purity by HPLC: 98%, mp 179.5 °C.

4.2.5. 7-(Ethyloxymorpholine)-1-methyl-β-carboline (3o)

Compound **3o** was obtained from a solution of harmol (0.440 g, 1.401 mmol), cesium carbonate (3.000 g, 9.208 mmol) and 4-(2-chloroethyl)morpholine hydrochloride (0.650 g, 3.493 mmol) in 10 mL of DMF. The reaction mixture was heated at 60 °C for 24 h. The crude product was purified by column chromatography (dichloromethane/methanol 90:10% v/v).

Yield 38%, R_f = 0.42 (DCM/EtOH/NEt_3 8:2:0.2). ^{1}H NMR ($CDCl_3$) δ: 2.61 (t, J = 4.6 Hz, 4H, CH_2 (morpholine)), 2.79 (s, 3H, CH_3), 2.86 (t, J = 5.7 Hz, 2H, O–CH_2–CH_2), 3.75 (t, J = 4.6 Hz, 4H, CH_2 (morpholine)), 4.20 (t, J = 5.7 Hz, 2H, O–CH_2), 6.90 (dd, J_{6-5} = 8.7 Hz, J_{6-8} = 2.3 Hz, 1H, H-6), 6.96 (d, J_{8-6} = 2.1 Hz, 1H, H-8), 7.70 (d, J_{4-3} = 5.3 Hz, 1H, H-4), 7.95 (d, J_{5-6} = 8.7 Hz, 1H, H-5), 8.31 (d, J_{3-4} = 5.5 Hz, 1H, H-3), 8.40 (s, 1H, N–H). ^{13}C NMR ($CDCl_3$) δ: 20.21 (CH_3), 54.22 (2 CH_2 (morpholine)), 57.71 (O–CH_2–CH_2), 66.33 (O–CH_2), 67.01 (2 CH_2 (morpholine)), 95.73 (C-8), 110.19 (C-6), 112.33 (C-4), 116.10 (C_q), 122.80 (C-5), 128.71 (C_q), 134.72 (C_q), 138.93 (C-3), 141.03 (C_q), 141.68 (C_q), 159.96 (C_q). MS: $[M+H]^+$ 312.1. Anal. Calcd for $C_{18}H_{21}N_3O_2 + 2H_2O$: C, 62.23%; H, 7.25%; N, 12.10%. Found: C, 62.72%; H, 7.22%; N, 11.82%. Purity by HPLC: 99%, mp 174.3 °C.

4.3. Single crystal X-ray crystallographic data of 3e

Single crystals of compound **3e** were obtained by slow evaporation of a solution of dichloromethane/ethanol at room temperature. X-ray intensities were collected on a Gemini Ultra R system (4-circle kappa platform, Ruby CCD detector) using Mo Kα radiation (λ = 0.71073 Å). Structure coordinates have been deposited at the Cambridge Crystallographic Data Center and allocated the deposition number CCDC-757790.

The structure was solved using Sir92 and refined by full matrix least squares on F^2 using the program Shelxl97.[19] All non-hydrogen atoms were treated anisotropically while a riding model was applied for the hydrogens. The trifluoromethyl group presents large ellipsoids. A disordered model with the trifluoromethyl group distributed over two sites could be defined. The disordered model was constrained to have chemically reasonable geometry, whereas restraints on the anisotropic displacement parameters were used for trifluoromethyl group.

*Compound **3e**:* Trigonal with hexagonal axes, R_3, a = 25.400(2) Å, b = 25.400(2) Å, c = 12.7030(10) Å, α = 90.00°, β = 90.00°, γ = 120.00°, V = 7097.5(10) Å^3, Z = 18, μ = 0.106 mm^{-1}, D_x = 1.298 g cm^{-3}, λ (Mo Kα) = 0.71073 Å, F(0 0 0) = 2880.0, T = 293(2) K, 1639 unique reflections (R_{int} = 0.0273), R_1 = 0.0617 for 1639 $F_o > 2\sigma(F_o)$, R_1 = 0.1117 for all data (3321), GOF = S = 0.978.

4.4. Enzymatic assays

The inhibitory potency against MAO-A and MAO-B was evaluated following a previously reported two steps methodology.[14] In the first step, human MAO-A or MAO-B enzyme is incubated with a luminogenic MAO substrate structurally related to the beetle luciferin. This luciferin derivative is converted by MAO into methyl ester luciferin. In the second step, the addition of the luciferin detection reagent allows to stop the MAO reaction but also to convert the methyl ester derivative into luciferin, thereby producing a luminescent signal. The amount of light produced is related to the activity of human MAO.

The MAO enzymes were derived from insect cells infected with recombinant baculovirus containing complementary DNA inserts for human MAO-A and MAO-B (Sigma–Aldrich, M7316 and M7441, respectively). The recombinant MAO enzymes were provided under microsomes at a protein concentration of 5 mg/mL.

The MAO-GLO™ two-step bioluminescent assay from Promega Corporation was performed in 96-wells plates Microlite 1+ (Thermo Fisher Scientific) at 37 °C. 25.0 μL of recombinant MAO enzyme (final reaction concentration of 0.5 U/mg) were first incubated with the test compound (12.5 μL) for 2 min 30 s. Secondly, 12.5 μL of substrate (final reaction concentration of 120 and 15 μM for MAO-A and MAO-B, respectively) were added to the mixture. Third, after 1 h of reaction, 50 μL of luciferin detection reaction (LDR) was added to the wells. The luminescent signal was measured 20 min after the addition of the LDR with a 96-wells luminometer Fluoroskan FL (Thermo Fisher Scientific).

Harmine and the β-carboline derivatives were tested in triplicate at 3 concentrations (10, 1 and 0.1 μM) against MAO-A and at 2 concentrations (10 and 1 μM) against MAO-B. IC_{50} and K_i values of the most promising compounds and harmine were evaluated. DMSO at a final reaction concentration of 12.5% was used as cosolvant to dissolve the test compounds in buffer (100 mM Hepes (pH 7.5) and 5% glycerol).

Percentages of inhibition at each concentration were calculated as follows: I (%) = 100 × {1 − (luminescent signal with test compound/luminescent signal without test compound)}. The inhibition percentages were plotted against the logarithms of the compound molar concentrations. The IC_{50} values were calculated from normalized sigmoidal dose–response non-linear regression curves using the GraphPad Prism 5.01 software and were expressed as means ± SD from triplicate experiments.

K_i values were determined from the IC_{50} values using the Cheng–Prusoff equation: $K_i = IC_{50}/(1 + [S]/K_m)$.[20] The aminopropylether analogue of methyl ester luciferin exhibited K_m values of 116.1 and 14.6 μM for MAO-A and MAO-B, respectively. K_i values were expressed as means with 95% confidence intervals in brackets.

4.5. Molecular docking

Molecular structure of compound **3e** obtained by X-ray crystallographic analysis was directly used for the docking simulations. Compound **3f** was drawn and minimized using CHARMm force field implemented in Discovery Studio 2.5. Docking of the inhibitors **3e** and **3f** into in the active site of the human MAO-A and MAO-B structures obtained through X-ray crystallography (2Z5X and 2V5Z, respectively),[10,15] was carried out using GOLD (version 3.2) program. The choice of these structures was guided by the quality of the crystallographic data and the fact that safinamide in 2V5Z X-ray crystallography was a non-covalent ligand crossing the entire binding site of MAO-B. As a consequence, the side chain of key residue ILE199 is oriented such as the 'entrance' and 'substrate' are merged. This structural prerogative is essential to model the binding of β-carboline derivatives that must be accommodated by both cavities. The interaction sphere in the docking was centered on the N5 atom of the flavin (FAD) in the catalytic site of the protein (MAO-A and MAO-B) and delimited by a 20 Å radius. Seven water molecules which occupy the space between the harmine and FAD were conserved from X-ray crystallography (2Z5X.pdb) into the MAO-A model. Into the MAO-B model, three conserved water molecules have been identified, which are buried in the vicinity of FAD and proved to be important for docking simulation of MAO-B selective ligand.[17] So these water molecules are kept inside the binding site as an integral part of the protein structure during the whole computational procedure. For the 25 genetic

algorithm (GA) runs performed, a total of 100,000 genetic operations were carried out on five islands, each containing 100 individuals. The niche size was set to 2, and the value for the selection pressure was set to 1.1. Genetic operator weights for crossover, mutation and migration were set to 95, 95 and 10, respectively. The scoring function used to rank the docking was Goldscore.

Acknowledgments

J. Reniers and R. Frederick thank the Belgian National Fund for Scientific Research (F.N.R.S.) for financial support and Ms. Bernadette Norberg for her assistance with the XRD analysis.

Supplementary data

Supplementary data associated with this article can be found, in the online version, at doi:10.1016/j.bmc.2010.11.041. These data include MOL files and InChiKeys of the most important compounds described in this article.

References and notes

1. Weyler, W.; Hsu, Y. P.; Breakefield, X. O. *Pharmacol. Ther.* **1990**, *47*, 391.
2. Edmondson, D. E.; Mattevi, A.; Binda, C.; Li, M.; Hubalek, F. *Curr. Med. Chem.* **2004**, *11*, 1983.
3. Abell, C. W.; Kwan, S. W. *Prog. Nucleic Acid Res. Mol. Biol.* **2001**, *65*, 129.
4. Grimsby, J.; Lan, N. C.; Neve, R.; Chen, K.; Shih, J. C. *J. Neurochem.* **1990**, *55*, 1166.
5. Tipton, K. F.; Boyce, S.; O'Sullivan, J.; Davey, G. P.; Healy, J. *Curr. Med. Chem.* **2004**, *11*, 1965.
6. Yamada, M.; Yasuhara, H. *Neurotoxicology* **2004**, *25*, 215.
7. Drukarch, B.; van Muiswinkel, F. L. *Biochem. Pharmacol.* **2000**, *59*, 1023.
8. Schapira, A. H. *Arch. Neurol.* **2007**, *64*, 1083.
9. Kim, H.; Sablin, S. O.; Ramsay, R. R. *Arch. Biochem. Biophys.* **1997**, *337*, 137.
10. Son, S. Y.; Ma, J.; Kondou, Y.; Yoshimura, M.; Yamashita, E.; Tsukihara, T. *Proc. Natl. Acad. Sci. U.S.A.* **2008**, *105*, 5739.
11. Ooms, F.; Frederick, R.; Durant, F.; Petzer, J. P.; Castagnoli, N.; Van der Schyf, C. J.; Wouters, J. *Bioorg. Med. Chem. Lett.* **2003**, *13*, 69.
12. Frederick, R.; Dumont, W.; Ooms, F.; Aschenbach, L.; Van der Schyf, C. J.; Castagnoli, N.; Wouters, J.; Krief, A. *J. Med. Chem.* **2006**, *49*, 3743.
13. Song, Y.; Wang, J.; Teng, S. F.; Kesuma, D.; Deng, Y.; Duan, J.; Wang, J. H.; Qi, R. Z.; Sim, M. M. *Bioorg. Med. Chem. Lett.* **2002**, *12*, 1129.
14. Valley, M. P.; Zhou, W.; Hawkins, E. M.; Shultz, J.; Cali, J. J.; Worzella, T.; Bernad, L.; Good, T.; Good, D.; Riss, T. L.; Klaubert, D. H.; Wood, K. V. *Anal. Biochem.* **2006**, *359*, 238.
15. Binda, C.; Wang, J.; Pisani, L.; Caccia, C.; Carotti, A.; Salvati, P.; Edmondson, D. E.; Mattevi, A. *J. Med. Chem.* **2007**, *50*, 5848.
16. Edmondson, D. E.; Binda, C.; Wang, J.; Upadhyay, A. K.; Mattevi, A. *Biochemistry* **2009**, *48*, 4220.
17. Novaroli, L.; Daina, A.; Favre, E.; Bravo, J.; Carotti, A.; Leonetti, F.; Catto, M.; Carrupt, P. A.; Reist, M. *J. Med. Chem.* **2006**, *49*, 6264.
18. Edmondson, D. E.; DeColibus, L.; Binda, C.; Li, M.; Mattevi, A. J. *Neural Transm.* **2007**, *114*, 703.
19. Sheldrick, G. M. *Acta Cryst.* **2008**, *A64*, 112.
20. Cheng, Y.; Prusoff, W. H. *Biochem. Pharmacol.* **1973**, *22*, 3099.